HIGH FIELD GRADIENT MULTI-POLE MAGNETS WITH PERMENDUR ALLOY FOR THE SPring-8 UPGRADE

Y. Okayasu*, C. Mitsuda, K. Fukami, K. Soutome, T. Watanabe and T. Nakamura
Japan Synchrotron Radiation Research Institute
1-1-1, Koto, Sayo-cho, Sayo-gun, Hyogo 679-5198, Japan

Abstract

One of the major goals for the SPring-8 upgrade is to reduce the beam emittance in the storage ring down the diffraction limit in the X-ray region using the same tunnel for the ring. In order to achieve the above goal while keeping the circumference the same, a magnet lattice with six bending magnets in a cell is designed. Although the final design has not been fixed yet, the designed lattice requires extremely strong magnetic fields, especially for the sextupole magnets, such as $\geq$10000 T/m^2. It is difficult to realize the value with the generic electromagnetic soft iron such as SUY alloys. As one of the possibilities to overcome the difficulty, we have been considering to introduce permendur alloy which is an iron based alloy with cobalt and vanadium. The saturated magnetic flux density of this alloy is about 1.4 times higher than the ordinary material. With these characteristics we expect to fulfill the requirements on the multi-pole magnets.

INTRODUCTION

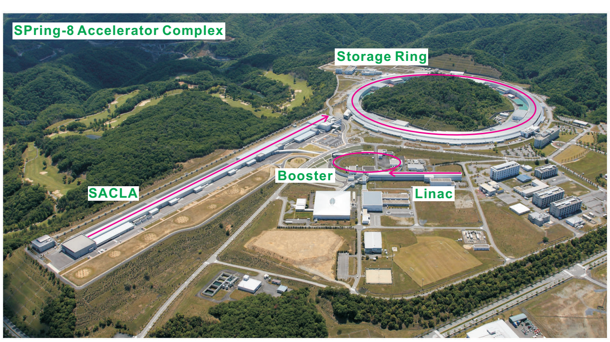

Figure 1: A bird's eye view of the SPring-8 accelerator complex. At present, SPring-8 consists of 1 GeV linac, 1 - 8 GeV booster synchrotron, 8 GeV storage ring and SACLA (XFEL). Normal operational beam energy of SACLA is designed as 8 GeV.

Approaching the beam emittance to the diffraction limit of light in the X-ray region (e.g., 10 pm·rad for 10 keV photon) is a key essential of the SPring-8 accelerator upgrade (SPring-8 II) with a restriction that the existing storage ring tunnel has to be reused. In order to realize such an ultra-low emittance in the storage ring, major efforts are allocated to the magnet lattice modification for the storage ring in SPring-8 II.

A site view of the SPring-8 accelerator complex is shown in Fig. 1. At present, SPring-8 consists of 1 GeV linac as an injector, 1 - 8 GeV booster synchrotron, 8 GeV storage ring and SACLA (XFEL). Normal operational beam energy of SACLA is designed as 8 GeV. In SPring-8 II, the operational beam energy of the storage ring is designed to be lowered from 8 to 6 GeV taking into account a required energy range of radiation spectrum. In addition, SACLA is also considered to be an injector candidate for the SPring-8 II storage ring.

In 1436 m circumference of existing storage ring, we plan to modify the present double-bend achromat lattice to a sextuple-bend one and to introduce bunch of strong focus multi-pole magnets in it. For example, 50 T/m and 10000 T/m^2 of higher field gradients with bore radius of ϕ26 mm are required for some quadrupole and sextupole magnets, respectively which are impossible to realize as far as using generic pure iron alloys such as JIS C 2504 SUY-0. Therefore, we plan to introduce permendur (Co-Fe) alloy, which is iron based alloy with cobalt and vanadium and enables to provide higher saturated field flux density, for the SPring-8 II multi-pole magnets pole pieces and the generic pure iron alloy for their return yokes. In fiscal year 2011, we plan to assemble a full scale mock-up of the sextupole magnet and to confirm to obtain required field gradient.

STORAGE RING LATTICE CONFIGURATION DESIGN

The SPring-8 II storage ring with 1436 mm circumference is divided into total 48 cells, 44 normal cells and 4 long straight cells. In the normal cells, we plan to install two short insertion devices (total length $\leq$ 500 mm, so called Mini-ID) in addition to the conventional one (total length $\leq$ 3000 mm, ID). On the other hand, one normal ID and an RF cavity unit is installed into the long straight cell. FIG. 2 shows a tentative design of the lattice configuration for the SPring-8 II normal unit cell and any correction magnets, vacuum components and beam diagnostics components are excluded. As shown in FIG. 2 (*blue*), we plan to adopt sextuple-bend achromat lattice, comparing to the present double-bend one. Also, a bunch of quadrupole (*green*) and sextupole (*brown*) magnets are installed, thus it is critical issue to keep installation rooms for other components such as correction magnets, vacuum pumps, gauges and BPMs. TABLE 1 summarizes primary parameters for

* okayasu@spring8.or.jp

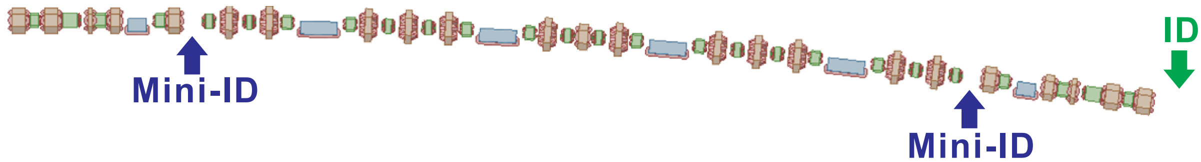

Figure 2: Top view of the lattice configuration design for the SPring-8 II normal unit cell. *Brown*, *green* and *blue* indicate sextupole, quadrupole and dipole magnets, respectively (*online*).

the entire SPring-8 II storage ring magnets.

Table 1: Primary parameters for the SPring-8 II storage ring magnets.

Field strength (abs.)	Effective field length [mm]	Number of magnets
Dipole [T]		
0.98	410	88
0.98	820	176
Quadrupole [T/m]		
36.6 ∼ 49.5	200	528
67.1	250	88
1.5 ∼ 49.8	300	456
13.6 ∼ 61.0	500	136
Sextupole [T/m^2]		
11385.8	100	88
1872.5	200	88
3962.2	250	88
1440.4 ∼ 8045.1	300	176
1237.1 ∼ 5967.9	400	572
Total		2484

MULTI-POLE MAGNET DESIGNS

In the following discussion, we focus on the sextupole magnet design procedure. In order to achieve the ultra-low emittance ring, SPring-8 II adopts ϕ26 mm bore radius comparing to ϕ92 mm of the present storage ring. In addition, as listed in TABLE 1, some required field gradients of the multi-pole magnets are too high (5 ∼ 27 times higher) as far as utilizing the generic magnetic iron alloys, thus we consider to introduce the Co-Fe alloy for such multi-pole magnets pole pieces. For return yokes, we adopt the generic magnetic iron alloys in order to keep production costs down. Indeed, one quadrupole magnet prototype for the J-PARC linac accelerator has been assembled and confirmed to obtain its required performance while its bore radius is ϕ17 mm[1]. Before starting the sextupole magnet design, we measured and compared B-H curves of the Co-Fe alloys with three different Co content rates, 5, 25 and 49 wt% as shown in FIG. 3[2]. From FIG. 3, it is found that rise rate in B-H curve is faster as Co content rate is lower, however filed flux density of 5 wt% Co composite is lower comparing to 25 and 49 wt% composites in entire range. In general, the Co-Fe alloy with higher Co wt% is more expensive, deteriorated its strength and its magnetostriction is more remarkable, however, ramp-up time is shorter. In this study, we designed full scale sextupole magnet mock-up as shown in FIG. 4 with 25 wt% Co of the Co-Fe alloy pole piece and the generic magnetic iron alloy for the return yoke. And the Cartesian coordinates are defined as described in FIG. 4, coordinate center is located at the mass center of the magnet.

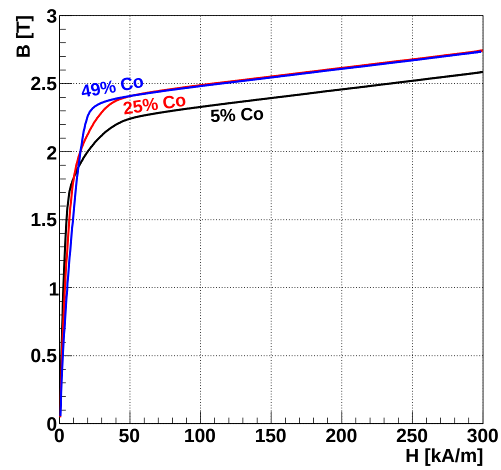

Figure 3: Measured B-H curves comparison with 5 (*black*), 25 (*red*) and 49 wt% (*blue*) Co of the Co-Fe alloys.

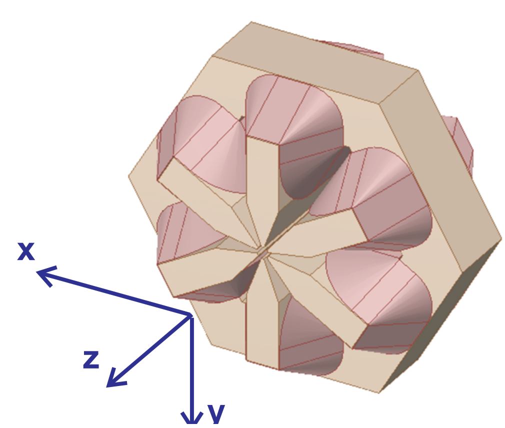

Figure 4: Schematic view of the sextupole magnet with effective field length of 400 mm.

As discribed in FIG. 2, saving installation space for other accelerator components, such as BPMs, vacuum pumps, gauges and even correction magnets, are critical issue, thus we adopt saddle shape coil as discribed in FIG. 4. Field gradient at the magnet center, inductance and saturations are calculated with the assumed sextupole moddel as described in FIG. 4 by CST MICROWAVE STUDIO®. Here, "Steel-1010" is assumed for the return yoke material which is generally used for the magnetic soft iron. In addition, we assumed 25 coil turns / pole with 75 A for the model.

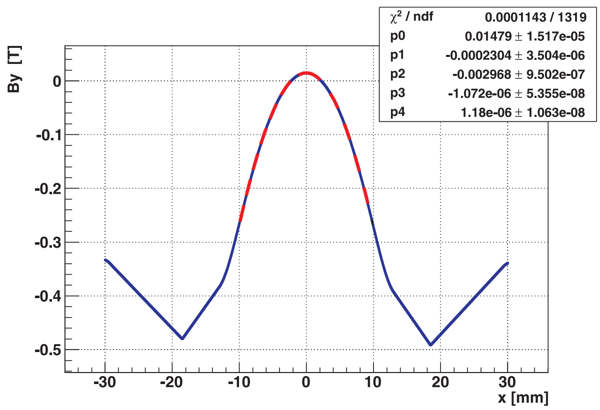

Figure 5: Calculated field flux density (B_y, *blue-solid*) along x-axis and fitting result (*red-dashed*).

Field flux density (B_y) along the x-axis is calculated and fitted with the 4th linear coupling function as shown in FIG 5. From FIG 5, the filed gradient ($D(x)$) at the mass center is found to be satisfied the maximum design value.

$$D(x=0) \equiv 2 \times \left.\frac{d^2 B_y}{dx^2}\right|_{x=0} \cong -5935.64 \quad [\mathrm{T/m^2}] \quad (1)$$

Furthermore, a flatness of the field gradient :

$$\Delta D(x) = \frac{D(x) - D(x=0)}{D(x=0)} \quad (2)$$

is evaluated to be $\Delta D(x) \leq 3.0 \times 10^{-3}$ ($|x \text{ [mm]}| \leq 5$) without sim shape optimization. Field flux distribution (absolute value) of the entire sextupole model is shown in FIG. 6. Maximum absolute flux is estimated to be 2.49 [T/m^2]. Finally, we summarize a specifications for the high field gradient sextupole mock-up in TABLE 2.

Table 2: Specifications for the high field gradient sextupole mock-up.

Effective field length	0.4 m
Coil turns per pole	25
Current per turn	75 A
Coil cross section	4.4×10^{-5} m^2
Coil length per turn (ave.)	0.7 m
Magnetomotive force	1875 A·turn/pole
Inductance	29.7 mH

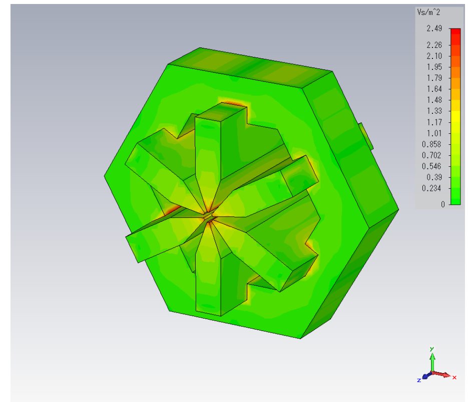

Figure 6: Calculated field flux density (|B|) distribution of the entire sextupole model.

FUTURE PLAN

As discussed above, the field gradient flatness for the present model is calculated to be 3.0×10^{-3} around the magnet mass center ($|x \text{ [mm]}| \leq 5$) while our end goal is $\leq 10^{-4}$, thus further sim shape optimization is required. Also, we are assembling a blocked sextupole prototype which is based on the specification as listed in TABLE 2 while the production one is considered to be layered. With the prototype, we plan to start the field measurement and to estimate its ramp-up time, magnetostrictive effect and so on by March 2012.

SUMMARY

In the SPring-8 II, we aim to reduce the storage ring beam emittance down the diffraction limit in the X-ray region with the existing ring tunnel, which is one of the major goal for the next upgrade. In addition, the operational beam energy of the storage ring is designed to be lowered from 8 to 6 GeV and bore radius is also required to be shrinked from the present ϕ92 mm to ϕ26 mm. According to these above backgrounds and the goal, we plan to modify the present double-bend achromat lattice to a sextuple-bend one and to introduce a bunch of very strong focus multi-pole magnets in it. Some field gradients are very high which is unable to realize with the generic magnetic soft iron alloy. Thus, we introduce the Co-Fe alloy for such multi-pole magnets' pole pieces. We design the sextupole prototype and proceed numerical analysis for a model, and confirm to obtain a required field gradient. Also, we are assembling the prototype based on parameters which are optimized by the numerical analysis and plan to start the field measurement, ramp-up time estimation and so on by March 2012.

REFERENCES

[1] E. Takasaki et. al., ASN-474, March 4, 2004

[2] Tohoku Steel Co., LTD., private communications.